Journal of
Ceramic Science
and Technology

J. Ceram. Sci. Technol., **17** [3] 255-262 (2026)
DOI: 10.4416/JCST2026-00009
available online at: http://www.ceramic-science.com
© 2026 Göller Verlag

Effect of Ultrafast Fiber Laser, Diode Laser, and Airborne Particle Abrasion on Surface Topography and Repair Bond Strength of Cerasmart Flexible Hybrid Ceramic: An *In Vitro* Comparative Study

S. Alresayes, E.M. Alhamdan*

Department of Prosthetic Dental Sciences, College of Dentistry,
King Saud University, Riyadh 11475, Saudi Arabia.

received June 9, 2026; received in revised form July 5, 2026; accepted July 9, 2026

Abstract

This *in vitro* study evaluated surface topography, roughness (R_a), and repair bond strength (RBS) of Cerasmart flexible hybrid ceramic blocks (FHBC) after conditioning with airborne particle abrasion (APA), diode laser (DL), and ultrafast fiber laser (UFL) irradiation versus an untreated control. 104 disc-shaped specimens were randomly allocated into four groups (n = 26): Group 1: control; Group 2: APA (50 μm Al_2O_3, 2.5 bar, 10 mm, 15 s); Group 3: DL (810 nm, 1.0 W, 33.5 J/cm², 60 s); Group 4: UFL (1 064 nm, 20 W, 100 kHz, 1.820 J/cm², 7 s). R_a was measured via contact profilometry; topography via scanning electron microscopy. RBS was assessed using shear bond strength (SBS) testing (n = 10/group) after silane application, universal adhesive, and composite buildup, followed by thermocycling (10 000 cycles, 5 – 55 °C). Failure modes were adhesive, cohesive, or admixed. Data were analyzed using one-way ANOVA and Tukey's HSD ($p < 0.05$). All protocols produced significantly higher R_a and RBS than the control. UFL yielded the highest values (R_a: 2.18 ± 0.22 μm; RBS: 13.30 ± 1.76 MPa). Group 1 exhibited the lowest R_a (0.45 ± 0.08 μm) and RBS (5.20 ± 0.91 MPa). Ultrafast laser irradiation is a promising, thermally safe alternative to APA for intraoral conditioning of FHC restorations before repair.

Keywords: Flexible hybrid ceramic, Cerasmart; surface conditioning, ultrafast fiber laser, diode laser, airborne particle abrasion, repair bond strength, surface roughness

I. Introduction

The growing demand for esthetic and durable indirect restorations has driven the development of hybrid ceramics (HBCs) or resin-matrix ceramics (RMCs) as a clinically viable alternative to conventional feldspathic porcelains and glass-ceramics, which, despite their optical superiority, remain limited by inherent brittleness and susceptibility to catastrophic fracture under occlusal loading [1,2]. HBCs incorporate a highly cross-linked polymer matrix reinforced with a high volume fraction of ceramic fillers, combining the esthetics of ceramics with the resilience, machinability, and chairside reparability of resin composites [3]. Their dentin-like elastic modulus facilitates favorable stress distribution, reduces restoration fracture risk, and minimizes opposing tooth wear [4]. Compatibility with resin-based luting agents and capacity for chairside repair further enhance clinical longevity, positioning HBCs as a versatile option for inlays, onlays, veneers, and single-unit crowns [5]. Among commercially available systems, Cerasmart (GC Corporation, Tokyo, Japan) has attracted considerable research interest. This flexible hybrid ceramic (FHBC) comprises a highly cross-linked UDMA/DMA co-polymer matrix reinforced with 71 wt% silica and barium glass-ceramic fillers, engineered to optimize the balance between mechanical performance and esthetic fidelity [6].

Though HBCs have gained considerable clinical acceptance, they remain susceptible to fracture, chipping, and surface degradation over time, necessitating reliable intraoral repair protocols to preserve restoration longevity and avoid complete replacement [7]. Numerous repair protocols have been proposed to enhance repair bond strength (RBS) primarily by increasing surface roughness (R_a) to promote micromechanical interlocking at the adhesive interface [8]. Among these, airborne particle abrasion (APA) with aluminum oxide particles is widely regarded as the gold standard for HBC surface conditioning before intraoral repair, owing to its capacity to effectively roughen the substrate surface and enhance resin wettability [9]. However, considerable debate persists in the literature regarding the optimal particle size, application pressure, and tip-to-surface distance required to achieve predictable and reproducible outcomes [9,10]. Additionally, APA presents several challenges, including potential health risks associated with aerosol generation, the risk of substrate damage, and environmental concerns [11]. Consequently, it is advisable to investigate alternative surface

* Corresponding author: ealhamdan@ksu.edu.sa

conditioning methods that pose fewer risks to both the restorative material and the clinical environment.

Lasers have been extensively employed to pretreat dental materials owing to their adaptability and high degree of controllability [12,13] Among available laser systems, the diode laser has attracted significant interest in dentistry [14]. Operating at wavelengths of 810–980 nm in the near-infrared spectrum, it delivers millimeter-level precision and produces controlled photothermal effects upon ceramic surfaces [15,16]. Notably, a thorough review of the literature reveals no published study evaluating diode laser irradiation specifically as a surface conditioning modality for flexible HBC in respect of R_a and repair bond strength.

Conventional lasers used in dental and materials applications operate with relatively long pulse durations in the microsecond-to-millisecond range, or in continuous wave mode. While these systems produce surface modification through photothermal and thermomechanical mechanisms, they share a critical limitation: uncontrolled thermal damage to the surrounding substrate [17,18]. In contrast, ultrafast fiber laser (UFL) systems have emerged as a more technologically advanced alternative. Operating at exceptionally high repetition rates, these systems reduce processing time, enhance ablation efficiency, and substantially limit the thermal and mechanical damage commonly associated with conventional long-pulse laser systems [19,20] Emerging evidence suggests that UFL irradiation holds promise in improving the bond strength between titanium and acrylic resin or resin cement, while also demonstrating effectiveness in creating surface roughness on zirconia substrates [21]. However, information on its effect on R_a and the bond strength of HBCs is still scarce, necessitating future inquiry.

The present study was formulated on the null hypotheses that surface conditioning of Cerasmart-FHBC with APA, DL, and UFL irradiation would produce no statistically significant difference in R_a and no changes in surface topography relative to the untreated control. Also, RBS of Cerasmart-FHBC following these conditioning protocols (APA, DL, and UFL) would be comparable to that of the unconditioned group. Accordingly, the study aimed to evaluate and compare surface topography, R_a, and RBS of Cerasmart FHBC subjected to different surface conditioning protocols.

II. Materials and Methods

This *in vitro* investigation was designed and executed in full conformity with the ethical guidelines outlined in the Declaration of Helsinki [22]. All experimental procedures were carried out under controlled and standardized laboratory conditions throughout the study.

Sample size calculation: The minimum adequate sample size was established using G*Power (version 3.1.9.7; Franz Faul, University of Kiel, Germany). Power analysis was conducted based on a one-way ANOVA framework encompassing four independent groups. Input parameters included a large anticipated effect size (Cohen's f = 0.50), a two-tailed alpha level set at 0.05, and a target statistical power of 80 %. These calculations indicated that a minimum of 26 specimens per group would be sufficient to detect meaningful between-group differences with adequate precision [23,24]. Accordingly, each group was subdivided for specific outcomes: eight specimens were designated for surface topographic evaluation and scanning electron microscopy (SEM), eight for quantitative R_a assessment, and ten for RBS testing.

Specimen preparation: Cerasmart CAD-CAM ceramic blocks (shade A2, size 14; GC Corp., Tokyo, Japan) were sectioned into 104 standardized disc-shaped specimens (10 mm diameter × 3 mm thickness) using a water-cooled low-speed diamond saw (Isomet 1000; Buehler, Lake Bluff, IL, USA). All sectioning was performed under continuous water irrigation to prevent thermal damage and dehydration artifacts. One surface of each specimen was wet-polished through ascending grades of silicon carbide abrasive paper (600, 800, 1 000, and 1 200 grit; Buehler) under running water for 60 seconds per grade to create a standardized, reproducible substrate surface. Following polishing, all specimens were ultrasonically cleaned in distilled water for 10 minutes (Branson 3800; Branson Ultrasonics, Brookfield, CT, USA), air-dried, and stored in distilled water at 37 °C until surface treatments were performed [25,26].

Random group allocation: All specimens were randomly allocated into four experimental groups (n = 26 per group) using a computer-generated random number sequence (Research Randomizer, Version 4.0; www.randomizer.org). Groups were designated as follows:

Surface conditioning protocols

Group 1: Control (No Surface Treatment): Specimens received no surface conditioning. The polished surface was rinsed with distilled water, gently air-dried, and used directly for subsequent testing procedures.

Group 2: APA: The polished FHBC surface was conditioned by means of airborne particle abrasion using 50 µm aluminum oxide particles (Cobra; Renfert GmbH, Hilzingen, Germany) delivered at a pressure of 2.5 bar from a distance of 10 mm perpendicular to the specimen surface for 15 seconds using a slow, circular motion. Following APA, specimens were ultrasonically cleaned in distilled water for 5 minutes and air-dried for 30 seconds prior to further processing [27].

Group 3: Diode Laser*:* Specimens were irradiated using a near-infrared diode laser (SiroLaser Blue; Dentsply Sirona, Bensheim, Germany) operating at a wavelength of 810 nm, with the following parameters: power output 1.0 W, continuous-wave mode, fiber-optic tip diameter 0.4 mm, tip-to-surface distance 1 mm (perpendicular orientation), irradiation time 60 seconds, and energy density (fluence) 33.5 J/cm². Irradiation was delivered using a standardized scanning motion along parallel horizontal lines at a scan spacing of 0.5 mm to ensure uniform surface coverage. Specimens were subsequently ultrasonically cleaned in distilled water for 5 minutes and air-dried for 30 seconds [3].

Group 4: UFL: Specimens were irradiated using an ytterbium-doped nanosecond fiber laser device (FiberLAST Inc., Ankara, Turkey) with a wavelength of 1 064 nm. Application parameters were as follows:

100 kHz repetition rate, 20 W output power, 1 mJ pulse energy, pulse duration 100 ns, and 7 mm spot size; fluence 1.820 J/cm²; irradiance 260 W/cm²; irradiation time 7 seconds. The system generates a 7-mm-diameter beam focused to a 20-µm spot area. The focal point is determined independently of the operator via the integrated lens system, with distance settings adjustable manually or automatically. A collimator with back-reflection protection was employed to safeguard the material surface. The internal air-cooling system of the laser device was utilized throughout irradiation to minimize thermal effects [19].

Surface roughness assessment: Surface roughness of all conditioned specimens (n = 8 per group) was measured using a contact profilometer (MarSurf PS1; Mahr GmbH, Göttingen, Germany). Three measurements were recorded per specimen at different locations, and the mean arithmetic average surface roughness (R_a, µm) was calculated. A cut-off wavelength (λ_c) of 0.8 mm and an evaluation length of 4.0 mm were applied throughout, in accordance with ISO 4287 standards [28].

Surface topography analysis (SEM): Eight randomly selected specimens from each group were examined by means of scanning electron microscopy (SEM; JEOL JSM-6380LV; JEOL Ltd., Tokyo, Japan) to characterize surface topography following conditioning. Specimens were mounted on aluminum stubs, sputter-coated with gold-palladium alloy, and examined at an accelerating voltage of 15 kV at magnifications of 500×, 1 000×, and 5 000×. Representative micrographs were captured from each specimen to document surface morphological changes induced by each conditioning protocol [29].

Repair Bond Strength Testing

Silane and adhesive application: Following surface conditioning, ten specimens from each group received standardized chemical treatment before composite buildup. A silane coupling agent (Monobond Plus; Ivoclar Vivadent, Schaan, Liechtenstein) was applied to the conditioned surface using a microbrush and allowed to react for 60 seconds under ambient conditions, followed by gentle air-thinning. A universal adhesive (Scotchbond Universal; 3M ESPE, St. Paul, MN, USA) was subsequently applied in a scrubbing motion for 20 seconds, air-thinned for 5 seconds, and light-cured for 10 seconds at 1 000 mW/cm² (Bluephase Style; Ivoclar Vivadent).

Composite buildup: Composite resin restoration was accomplished using a micro-hybrid formulation (Filtek Z250; 3M ESPE, St. Paul, MN, USA) applied in an incremental layering technique. Two successive 2-mm layers were deposited within a standardized Tygon tube mold (internal diameter: 4 mm; height: 4 mm), with each increment independently polymerized for 20 seconds at an irradiance of 1 000 mW/cm². To ensure procedural consistency and minimize operator-related variability, all composite restorations were completed by a single trained and calibrated operator throughout the study.

Artificial aging: Before accelerated aging, all fabricated specimens were immersed in distilled water and maintained at 37 °C for 24 hours. Thermocyclic aging was subsequently carried out using a thermocycler (THE-1100; SD Mechatronik, Feldkirchen-Westerham, Germany). Specimens underwent 10 000 thermal cycles alternating between water baths set at 5 °C and 55 °C, simulating the thermal fluctuations experienced in the oral environment. Each temperature bath maintained a dwell time of 30 seconds, with an inter-bath transfer interval of 10 seconds [30, 31].

Repair bond strength testing: Repair bond strength was quantified by means of shear bond strength (SBS) testing, conducted using a calibrated universal testing machine (Zwick/Roell Z005; Zwick/Roell, Ulm, Germany) equipped with a 5-kN load cell. Each specimen was rigidly secured within a custom-fabricated metal jig to ensure consistent load application and prevent specimen displacement during testing. A stainless-steel rod with a chisel-shaped blade was positioned at the composite-ceramic bonded interface, with the blade edge oriented parallel to the bonded surface and perpendicular to the direction of applied force, in accordance with previously validated shear testing configurations. A compressive shear load was applied at a standardized crosshead displacement rate of 0.5 mm/min under ambient conditions until interfacial failure occurred. The maximum load at failure (N) was continuously recorded with the integrated data acquisition system. RBS values (MPa) were subsequently calculated by dividing the recorded peak failure load by the bonded cross-sectional area, as determined from the internal diameter of the Tygon mold using the following expression: [10]

$$\text{SBS (MPa)} = \text{F (N)} \div \text{A (mm}^2\text{)}$$

where F denotes the maximum load at failure, and A represents the bonded interfacial area, calculated as πr^2, where r is the radius of the bonded surface.

Failure mode analysis: All debonded specimens were examined under a stereomicroscope (Leica M80; Leica Microsystems, Wetzlar, Germany) at ×40 magnification by two blinded, calibrated examiners. Failure modes were classified as adhesive (failure at the composite-ceramic interface), cohesive (failure within either the composite or ceramic substrate), or admixed (combination of both). Inter-examiner agreement was quantified by Cohen's kappa coefficient (0.91) [28].

Statistical analysis: Before inferential analysis, the distribution of all continuous outcome variables was assessed for normality using the Shapiro-Wilk test, and variance homogeneity was confirmed through Levene's test. As all datasets fulfilled the assumptions underlying parametric analysis, one-way ANOVA was employed to identify statistically significant differences in surface roughness and repair bond strength across the four experimental groups. Where significant main effects were identified, pairwise intergroup comparisons were conducted using Tukey's post hoc test. The threshold for statistical significance was set at $p < 0.05$ for all analyses.

III. Results

***R_a* analysis:** Fig. 1 presents the mean R_a values of flexible hybrid ceramics after different conditioning protocols. The highest mean R_a value was recorded in the UFL-irradiated group (2.18 ± 0.22 µm), while the

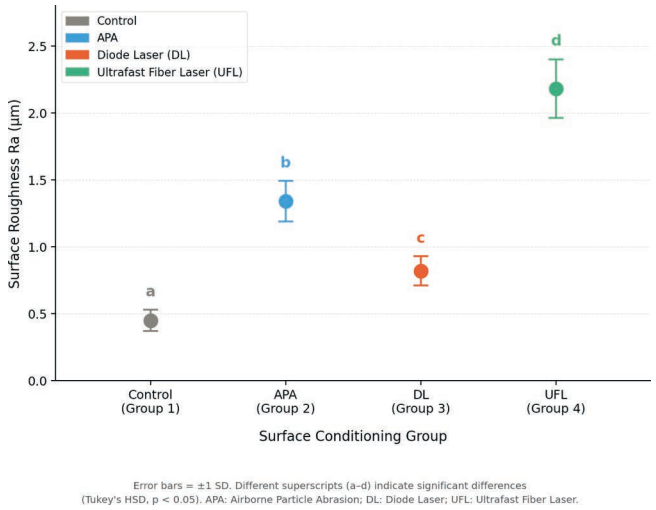

Fig. 1: Scatter plot of mean R_a values with ±1 SD error bars across surface conditioning groups.

untreated control group exhibited the lowest R_a value (0.45 ± 0.08 µm). Post-hoc Tukey HSD analysis confirmed statistically significant differences across all pairwise intergroup comparisons ($p < 0.05$). The UFL group recorded significantly higher R_a than all other groups. APA (1.34 ± 0.15 µm) produced significantly greater surface roughness than both the DL (0.82 ± 0.11 µm) and control groups. The DL group, while significantly rougher than the untreated control, produced significantly lower R_a than both UFL and APA ($p < 0.05$).

Repair bond strength: Table 1 presents the repair bond strength values of flexible hybrid ceramics after different conditioning protocols. The highest mean RBS was recorded in the UFL-irradiated group (13.30 ± 1.76 MPa), while the untreated control group exhibited the lowest RBS value (5.20 ± 0.91 MPa). Post-hoc Tukey HSD analysis confirmed statistically significant differences across all pairwise intergroup comparisons ($p < 0.05$). The UFL group recorded significantly higher RBS than all other groups. APA (10.85 ± 1.42 MPa) produced significantly greater RBS than both the DL (7.80 ± 1.13 MPa) and control groups ($p < 0.05$). The DL group, while demonstrating significantly higher RBS than the untreated control, remained significantly inferior to both UFL and APA ($p < 0.05$).

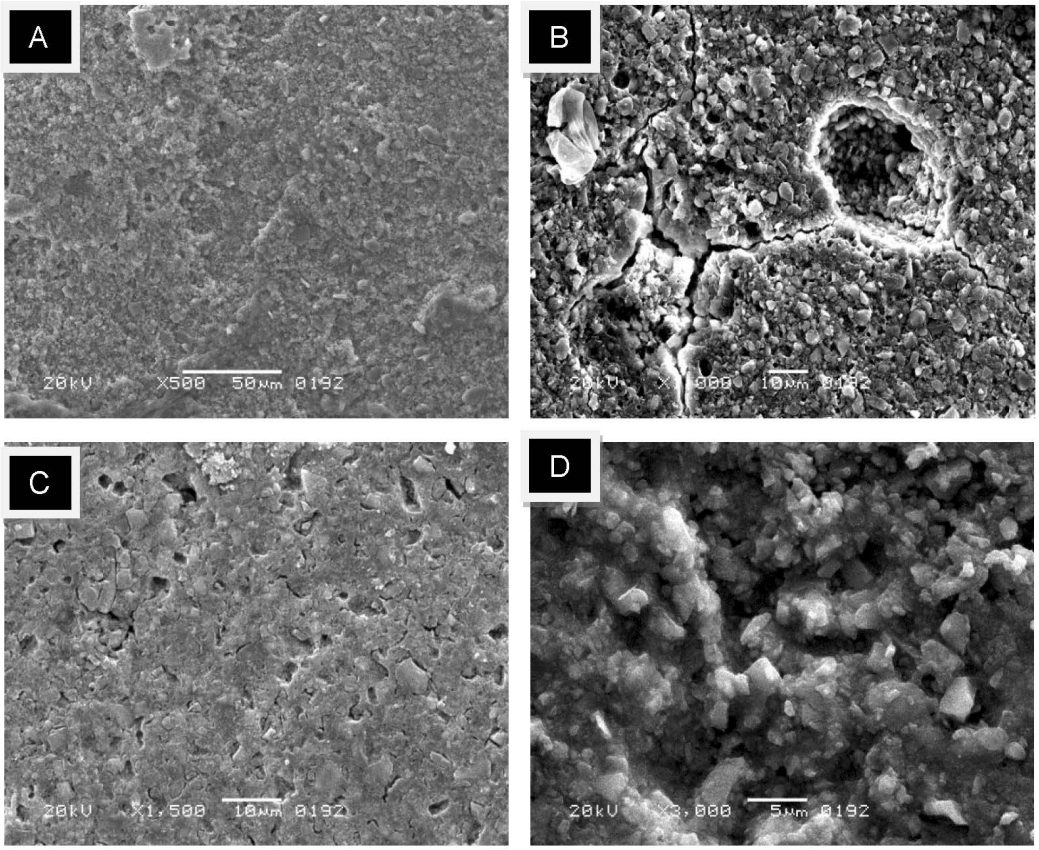

A Control — untreated surface; smooth, homogeneous texture

B APA (Airborne Particle Abrasion) — irregular surface with craters and micro-cracks

C DL (Diode Laser) — pitted surface with increased microporosity

D UFL (Ultrafast Fiber Laser) — highly roughened surface with granular texture and maximum Ra

APA: Airborne Particle Abrasion; DL: Diode Laser Irradiation; UFL: Ultrafast Fiber Laser Irradiation. Scale bars are indicated in each panel.

Fig. 2: SEM images of Cerasmart flexible hybrid ceramic surfaces after different surface conditioning protocols.

Table 1: RBS of flexible hybrid ceramics after different surface conditioning protocols

Groups	RBS (MPa) Mean ± SD	Significance!
Group 1: Control	5.20 ± 0.91 [a]	p < 0.05
Group 2: APA	10.85 ± 1.42 [b]	
Group 3: DL	7.80 ± 1.13 [c]	
Group 4: UFL	13.30 ± 1.76 [d]	

! ANOVA
APA: Airborne Particle Abrasion; DL: Diode Laser Irradiation; UFL: Ultrafast Fiber Laser Irradiation. Different superscript letters denote statistically significant differences between all groups by Tukey's HSD test (p < 0.05)

Failure mode analysis: Fig. 3 presents the fracture mode distribution across groups. Group 4 (UFL) predominantly demonstrated cohesive failure (60 %). Groups 2 (APA) and 3 (DL) exhibited a higher proportion of admixed fractures (50 % and 40 %, respectively). Group 1 (control) displayed the highest proportion of adhesive failures (50 %).

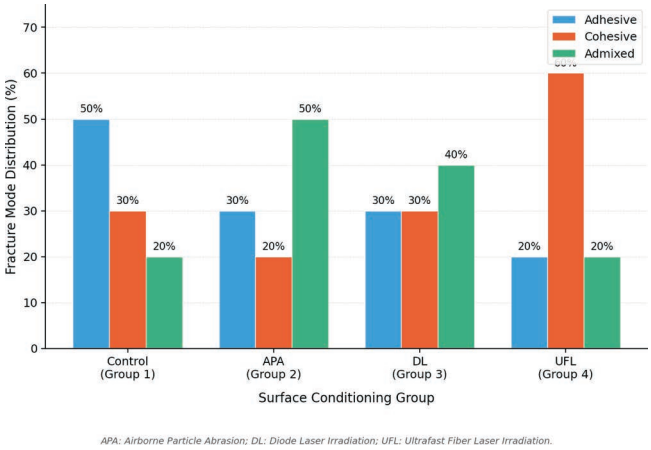

Fig. 3: Fracture mode distribution (%) of flexible hybrid ceramic specimens across surface conditioning groups.

IV. Discussion

The present study was formulated on the null hypotheses that surface conditioning of Cerasmart FHBC with APA, DL, or UFL irradiation would produce no statistically significant difference in R_a and surface topography relative to the untreated control, and that RBS following these conditioning protocols would be comparable to that of the unconditioned group. Based on the findings, it can be observed that all the pretreatment groups demonstrated significantly better R_a and RBS than the control, rejecting both the null hypotheses. UFL-irradiated specimens exhibited the highest R_a scores and maximum RBS outcomes across all experimental conditions. These findings align with those of Aladağ and coworkers, who reported that UFL irradiation represents a promising method for improving SBS of flexible hybrid ceramics without causing thermal damage to the substrate [32,33]. Likewise, Demirtag and Culhaoglu demonstrated that UFL (300 mW, 1 kHz) roughened the surface of resin matrix ceramics more effectively than hydrofluoric acid and that the highest SBS values were obtained with the UFL + silane combination [34], Kara *et al.* applied different laser systems to zirconia and reported that UFL (400 mW, 1 kHz) significantly increased R_a and SBS values [35], The mechanistic basis of these outcomes is that UFL induces surface evaporation without bulk melting of the substrate, owing to the highly focused, ultrashort pulse energy. As no sustained thermal effect occurs during treatment, crack formation and thermal damage are minimized relative to conventional laser systems [19,32]. At the microstructural level, the ytterbium-doped fiber laser (YbFL; λ = 1 064 nm) enhances R_a through selective photomechanical ablation: near-infrared photons are preferentially absorbed by the organic UDMA/DMA polymer matrix, inducing selective resin phase ablation while preserving the silica and barium glass filler network, thereby exposing filler particle protrusions and generating micro-irregular surface topography [32]. Concurrently, interference between the incident beam and surface electromagnetic waves produces laser-induced periodic surface structures (LIPSS) nanoscale ripple architectures superimposed on microscale ablation craters, collectively establishing a hierarchical micro-nano surface texture [36]. In accordance with Wenzel's theory, this roughness increase amplifies the intrinsic hydrophilicity of the ceramic surface, reducing adhesive contact angle, promoting capillary infiltration of resin monomers, and thereby enhancing repair bond strength [37]

APA produced significantly higher R_a and RBS than DL irradiation and the untreated control, though significantly inferior to UFL ($p < 0.05$). Upon particle impact, abrasive action non-selectively affects both the organic polymer matrix and ceramic filler phase, removing the surface resin-rich layer and exposing underlying silica and barium glass fillers to generate an irregular relief of sharp-edged peaks and deep valleys that substantially increase surface area available for adhesive infiltration and micromechanical interlocking [38,39]. In the present study, parameters of 50 µm Al_2O_3 particle size, 2.5 bar air pressure, 10 mm nozzle distance, and 15-second application time were deliberately selected to maximize R_a without inducing subsurface microcracking or compromising bulk mechanical integrity, a balance that likely accounts for the superior RBS values observed relative to both the DL-irradiated and untreated groups. These findings are consistent with those reported by Kim *et al.* [40]

DL irradiation produced significantly greater R_a and RBS than the untreated control but was significantly inferior to both APA and UFL ($p < 0.05$). The diode laser-hybrid ceramic interface remains understudied, with most published trials employing Er: YAG or Er, Cr: YSGG as surface conditioning modalities. Diode lasers operating at 810–980 nm demonstrate a characteristically low absorption coefficient for both water and hydroxyapatite [41]. Their photothermal effect is instead mediated by tissue and material chromophores, principally melanin, hemoglobin, and organic pigments, which

selectively absorb near-infrared photon energy, generating localized heat [42]. Within resin-containing materials, this energy is absorbed by organic constituents, including residual photoinitiators and polymer chains, while largely bypassing the inorganic ceramic phase [43]. Diode laser irradiation thus acts through photothermal ablation, selectively volatilizing the resin polymer phase of hybrid ceramics while leaving the ceramic filler partially exposed, creating micropitting and irregular surface topography that raises R_a values above baseline [44]. These outcomes are further supported by SEM findings; however, additional studies with variable parameter settings are required to confirm and optimize these observations.

The fracture mode distribution was consistent with the RBS hierarchy. UFL-irradiated specimens predominantly exhibited cohesive failure (60 %), a pattern recognized as indicative of bond strength values that approach or exceed the cohesive strength of the adherend or substrate. APA and DL groups demonstrated predominantly admixed failures (50 % and 40 %, respectively), reflecting intermediate bond quality with concurrent interfacial and cohesive breakdown. The control group displayed the highest proportion of adhesive failures (50 %), reflecting predominantly weak interfacial bonding. These observations are in agreement with findings reported by Maawadh *et al.* [3] and Falacho *et al.* [45] who noted that adhesive failure was predominant in groups with low repair bond values, while cohesive and admixed failure types characterized groups with superior adhesion.

Several limitations of the present investigation warrant consideration. The study was conducted under controlled *in vitro* conditions, and direct extrapolation to the clinical intraoral environment should be approached with caution. Although thermocycling with 10 000 cycles was employed to simulate approximately one year of intraoral aging, this model cannot fully replicate the complex oral milieu, including masticatory loading, salivary enzymatic activity, pH fluctuations, and cumulative occlusal fatigue. Shear bond strength was used as the sole mechanical testing modality; complementary approaches such as microtensile testing or cyclic fatigue loading would provide a more comprehensive characterization of interfacial durability. The study utilized a single RMC system (Cerasmart), limiting generalizability to other commercially available flexible hybrid ceramic blocks. Both laser groups were evaluated at fixed irradiation parameters, precluding the determination of optimized protocols; future dose-response investigations are warranted. The absence of atomic force microscopy (AFM) limits the characterization of nanoscale surface features, particularly LIPSS generated by the UFL system. Long-term clinical trials are ultimately necessary before definitive clinical recommendations can be established.

V. Conclusions

Ultrafast laser irradiation may represent a promising, thermally safe alternative to conventional airborne particle abrasion for intraoral surface conditioning of flexible hybrid ceramic restorations before repair. Parameter optimization studies and long-term randomized clinical trials are warranted to confirm the translational potential of this approach.

References

1 Alamoush, R.A., Silikas, N., Salim, N.A., Al-Nasrawi, S., Satterthwaite, J.D.: Effect of the composition of CAD/CAM composite blocks on mechanical properties, *Biomed. Res. Int.*, **2018**, 4893143, (2018).

2 Çelik, E., Sahin, S.C., Dede, D.Ö.: Shear bond strength of nanohybrid composite to the resin matrix ceramics after different surface treatments, *Photomed. Laser Surg.*, **36**, [8], 424 – 430, (2018).

3 Maawadh, A.M., Almohareb, T., Al-Hamdan, R.S., Al Deeb, M., Naseem, M., Alhenaki, A.M., Vohra, F., Abduljabbar, T.: Repair strength and surface topography of lithium disilicate and hybrid resin ceramics with LLLT and photodynamic therapy in comparison to hydrofluoric acid, *J. Appl. Biomater. Funct. Mater.*, **18**, (2020).

4 Jorquera, G., Mahn, E., Sanchez, J.P., Berrera, S., Prado, M.J., Stange, V.B.: Hybrid ceramics in dentistry: a literature review, *J. Clin. Res. Dent.*, **1**, [2], 1 – 5, (2018).

5 Alsunbul, H., Almutairi, B., Aljanakh, M., Abduljabbar, T.: Hybrid ceramic repair strength, surface roughness, and bond failure, using methylene blue-activated low-level laser therapy, carbon dioxide, and Ti:Al_2O_3 laser, *Photodiagnosis Photodyn. Ther.*, **43**, 103693, (2023).

6 Beltrami, Í.M., de Lima, C.C., do Nascimento, C.T., Gonçalves, J.G.P., Azarias, J.S., Bortoleto, A.L.F., Goiato, M.C., dos Santos, D.M.: Hybrid ceramics cementation protocols: scope review, *J. Clin. Exp. Dent.*, **16**, [9], e1138 – e1150, (2024).

7 Campos, F., Almeida, C.S., Rippe, M.P., De Melo, R.M., Valandro, L.F., Bottino, M.A.: Resin bonding to a hybrid ceramic: effects of surface treatments and aging, *Oper. Dent.*, **41**, [2], 171 – 178, (2016).

8 Jung, S.N., Rüttermann, S.: Influence of mechanical and chemical pre-treatments on the repair of a hybrid ceramic, *Dent. Mater.*, **38**, [7], 1140 – 1148, (2022).

9 Albakri, A.S.: Pretreatment of hybrid ceramics using alumina (Al_2O_3) nanoparticles, hydrofluoric acid, and holmium:YAG laser for optimizing surface roughness, shear bond strength, and topography, *J. Biomater. Tissue Eng.*, **13**, [12], 1133 – 1138, (2024).

10 Jung, S.N., Rüttermann, S.: Influence of mechanical and chemical pre-treatments on the repair of a hybrid ceramic, *Dent. Mater.*, **38**, [7], 1140 – 1148, (2022).

11 Alkhudhairy, F., AlFawaz, Y.F.: Pretreatment of hybrid ceramics using Ho:YAG, low-level laser therapy activated malachite green, and non-thermal plasma on surface roughness, bond strength, and color change, SEM and EDX analysis, *Ceramics*, **7**, [3], 944 – 957, (2024).

12 Alkhudhairy, F., Vohra, F., Naseem, M.: Influence of er,Cr:YSGG laser dentin conditioning on the bond strength of bioactive and conventional bulk-fill dental restorative material, *Photobiomodulation Photomedicine Laser Surg.*, **38**, [1], 30 – 35, (2020).

13 Aljamhan, A.S., Alrefeai, M.H., Alhabdan, A., Alzehiri, M.H., Naseem, M., Vohra, F., Alkhudhairy, F.: Interaction of zirconium oxide nanoparticle infiltrated resin adhesive with dentin conditioned by phosphoric acid and er,Cr:YSGG laser, *J. Appl. Biomater. Funct. Mater.*, **20**, (2022).

14 Labunet, A., Tonea, A., Kui, A., Sava, S.: The use of laser energy for etching enamel surfaces in dentistry – a scoping review, *Materials* (Basel), **15**, [6], 1988, (2022).

15 Alam, M.K., Almaeen, H.A.H., Alsunaydi, T.A.M., Alruwaili, D.H.J., Almutairi, T.F., Alanazi, H.M.A.: The use of lasers

in enhancing the bond strength of orthodontic brackets, *J. Pharm. Bioallied Sci.*, **16**, (Suppl 1), S524 – S526, (2024).

16 Aljamhan, A.S., Alrefeai, M.H., Alhabdan, A., Alhusseini, S.A., Farooq, I., Vohra, F., Naseem, M., Alkhudhairy, F.: Influence of er-cr-YSGG laser and photodynamic therapy on the dentin bond integrity of nano-hydroxyapatite containing resin dentin adhesive: SEM-EDX, micro-raman, micro-tensile, and FTIR evaluation, *Polymers* (Basel), **13**, [12], 1903, (2021).

17 Wilson, A., Jones, I., Salamat-Zadeh, F.: Laser surface modification of poly(etheretherketone) to enhance surface free energy, wettability and adhesion, *Int. J. Adhes. Adhes.*, **62**, 56 – 66, (2015).

18 Abu Hasna, A., Semmelmann, S., Feitosa, F.A., De Souza Andrade, D., Tay, F.R., Pucci, C.R.: Effect of Nd:YAG laser with/without graphite coating on bonding of lithium disilicate glass-ceramic to human dentin, *Int. J. Dent.*, **2021**, 6677159, (2021).

19 Ates, S.M., Korkmaz, F.M., Caglar, I.S., Duymus, Z.Y., Turgut, S., Bagis, E.A.: The effect of ultrafast fiber laser application on the bond strength of resin cement to titanium, *Lasers Med. Sci.*, **32**, (5), 1121 – 1129, (2017).

20 Ma, Z., Meng, F., Cui, Z., Chen, L., Zhang, C., Liu, C., Yu, T.: Surface formation mechanism in ultrasonic vibration assisted grinding dental zirconia ceramic process considering stochasticity of grits, *J. Mater. Res. Technol.*, **36**, 2718 – 2730, (2025).

21 Kerse, C., Kalaycıoğlu, H., Elahi, P., Çetin, B., Kesim, D.K., Akçaalan, Ö., Yavaş, S., Aşık, M.D., Öktem, B., Hoogland, H., Holzwarth, R., Ilday, F.Ö.: Ablation-cooled material removal with ultrafast bursts of pulses, *Nature*, **537**, (7618), 84 – 88, (2016).

22 Goodyear, M.D.E., Krleza-Jeric, K., Lemmens, T.: The declaration of helsinki, *Br. Med. J.*, **335**, (7621), 624 – 625, (2007).

23 Alshahrani, A., Alhamdan, R.S., Alsaqat, R.T., Alresayes, S., Al Rifaiy, M.Q., Almutairi, B.: Impact of lithium disilicate ceramic surface modifiers and resin cement of different viscosities on surface roughness and bond strength after artificial aging: a SEM assessment, *J. Ceram. Sci. Technol.*, **16**, [2], 37 – 44, (2025).

24 Almutairi, B., Al-Hamdan, R.S., Alresayes, S., Alsunbul, H., Alzahrani, K.M., Abduljabbar, T.: Impact of er,Cr:YSGG laser at different power outputs and hydrofluoric acid on the shear bond strength and color stability of lithium disilicate ceramic and hybrid ceramic, *J. Ceram. Sci. Technol.*, **16**, [2], 93 – 100, (2025).

25 Almohareb, T., Maawadh, A., AlDeeb, L., Alahdal, K., Alshamrani, A.S., Alrahlah, A.: Influence of high- and low-viscosity resin cement and artificial aging on bond integrity and surface roughness of lithium disilicate ceramics pretreated with Ho:YAG laser and nano-hydroxyapatite coatings, *J. Ceram. Sci. Technol.*, **16**, [1], 29 – 36, (2025).

26 Alhamdan, E.M.: Repair bond strength and surface roughness of zirconia ceramics treated via carbon dioxide laser, malachite green, and sandblasting. A lab-based study, *J. Ceram. Sci. Technol.*, **16**, [2], 85 – 92, (2025).

27 Prieto, M.V., Gomes, A.L.C., Martín, J.M., Lorenzo, A.A., Mato, V.S., Martínez, A.A.: The effect of femtosecond laser treatment on the effectiveness of resin-zirconia adhesive: an in vitro study, *J. Lasers Med. Sci.*, **7**, [4], 214 – 219, (2016).

28 Alkhudhairy, F., Vohra, F., Naseem, M., Owais, M.M., Amer, A.H.B., Almutairi, K.B.: Color stability and degree of conversion of a novel dibenzoyl germanium derivative containing photo-polymerized resin luting cement, *J. Appl. Biomater. Funct. Mater.*, **18**, (2020).

29 Aljamhan, A., Alkhudhairy, F.: Effect of pre-treatment techniques Nd:YLF laser, nano-HAp particles on surface roughness and repair bond strength of different-viscosity composite bonded to hybrid ceramics, *J. Ceram. Sci. Technol.*, **16**, [4], 263 – 268, (2025).

30 Alrabiah, M.A., Alkhudhairy, F.: Surface roughness and bond strength of PEEK posts: comparing chemical, mechanical, and laser methods, *Int. Dent. J.*, **76**, [3], 109535, (2026).

31 Alanazi, A., Naseem, M., Dehn, C., Abrar, E., Afzal, A.: Ho:YAG laser as a chemical-free alternative to sulfuric acid for PEEK surface conditioning: effect on surface roughness, shear bond strength, and adhesive system performance, *Int. J. Adhes. Adhes.*, **149**, 104372, (2026).

32 Aladağ, S.Ü., Ayaz, E.A.: Comparison of the effects of laser systems and cold atmospheric plasma on the surface roughness and shear bond strength of flexible hybrid ceramics, *Lasers Med. Sci.*, **39**, [1], 276, (2024).

33 Aladağ, S.Ü., Ayaz, E.A.: Repair bond strength of different CAD-CAM ceramics after various surface treatments combined with laser irradiation, *Lasers Med. Sci.*, **38**, [1], 51, (2023).

34 Demirtag, Z., Culhaoglu, A.K.: Surface roughness of ceramic-resin composites after femtosecond laser irradiation, sandblasting or acid etching and their bond strength with and without silanization to a resin cement, *Oper. Dent.*, **44**, [2], 156 – 167, (2019).

35 Kara, O., Kara, H.B., Tobi, E.S., Ozturk, A.N., Kilic, H.S.: Effect of various lasers on the bond strength of two zirconia ceramics, *Photomed. Laser Surg.*, **33**, [2], 69 – 76, (2015).

36 Wang, H., Hu, Y., Cong, W., Hu, Z.: A mechanistic model on feeding-directional cutting force in surface grinding of CFRP composites using rotary ultrasonic machining with horizontal ultrasonic vibration, *Int. J. Mech. Sci.*, **155**, 450 – 460, (2019).

37 Onda, T.: Theoretical investigation of wenzel and cassie wetting states on porous films and fiber meshes, *Langmuir*, **38**, [45], 13744 – 13752, (2022).

38 Prasad, H.A., Pasha, N., Hilal, M., Amarnath, G.S., Kundapur, V., Anand, M., Singh, S.: To evaluate effect of airborne particle abrasion using different abrasives particles and compare two commercial available zirconia on flexural strength on heat treatment, *Int. J. Biomed. Sci.*, **13**, [2], 93 – 103, (2017).

39 Okutan, Y., Kandemir, B., Gundogdu, Y., Kilic, H.S., Yucel, M.T.: Combined application of femtosecond laser and air-abrasion protocols to monolithic zirconia at different sintering stages: effects on surface roughness and resin bond strength, *J. Biomed. Mater. Res. Part B Appl. Biomater.*, **109**, [4], 596 – 605, (2021).

40 Kim, H.K., Ahn, B.: Effect of Al_2O_3 sandblasting particle size on the surface topography and residual compressive stresses of three different dental zirconia grades, *Materials* (Basel), **14**, [3], 610, (2021).

41 Fahim, S.Z., Ghali, R.M., Hashem, A.A., Farid, M.M.: The efficacy of 2780 nm er,Cr:YSGG and 940 nm diode laser in root canal disinfection: a randomized clinical trial, *Clin. Oral Investig.*, **28**, [3], 175, (2024).

42 Bornstein, E.: Near-infrared dental diode lasers: scientific and photobiologic principles and applications, *Dent. Today*, **23**, [3], 102 – 108, (2004).

43 Lagunov, V.L., Ali, B., Walsh, L.J., Cameron, A.B., Litvinyuk, I.V., Rybachuk, M., George, R.: Properties of zirconia, lithium disilicate glass ceramics, and VITA ENAMIC® hybrid ceramic dental materials following ultra-short femtosecond (30 fs) laser irradiation, *Appl. Sci.*, **14**, [17], 7641, (2024).

44 Usta Kutlu, İ., Yerliyurt, K.: The impact of various surface treatments and Er:YAG laser irradiation on the bond strength of resin matrix CAD/CAM ceramics to resin cement, *Lasers Med. Sci.*, **40**, [1], 201, (2025).

45 Falacho, R.I., Almeida, G., Ñaupari-Villasante, R., Marques, J.A., Caramelo, F., Blatz, M.B., Loguercio, A., Ramos, J.C.: Effect of different airborne-particle abrasion strategies on dentin bond strength: an in vitro study, *J. Esthet. Restor. Dent.*, **38**, [1], 173 – 184, (2025).